

Chapter 3

Review of Works on Semiconductor Annealing

3.1 Investigations of Annealing Effects on (In)GaAsN Materials

3.1.1 Blueshift of Optical Emission upon Annealing

Because of the intended applications to laser diodes (LD) of this group of materials, the photoluminescence (PL) properties of the (In)GaAsN materials was the most concerned and have been largely studied with various growth methods and annealing processes. Most of the results have found a blue shift effect upon annealing on the samples, such as, E. Tournie *et al.* [45] (2002), M. Kondow *et al.* [46] (2004) and B. Kudrawiec *et al.* [47] (2004). But there are different interpretations on the origin mechanisms of the blue shift, mainly:

The Diffusion There have been several reports on the PL blueshift of (In)GaAsN/GaAs QWs caused by the interdiffusion of the atoms in the alloys, Li *et al.* [48] studied strain-compensated GaInNAs/GaAsP quantum well structures and lasers which were grown by gas-source molecular beam epitaxy using a rf-plasma nitrogen radical beam source. With increasing RTA temperature, the PL peaks blueshift and broaden for all the QWs, they supposed this blueshift and broadening was due to the diffusion of In and N as well as P atoms at the QW interface.

Another example is the work carried out by B. Damimano *et al.* [49], in which conjugated effect of growth temperature and in situ thermal annealing on the photoluminescence properties of $\text{In}_{0.4}\text{Ga}_{0.6}\text{As}_{0.985}\text{N}_{0.015}/\text{GaAs}$ single quantum wells (SQW) were investigated. Their samples were grown by molecular-beam epitaxy (MBE) and annealed in situ at 700°C for 1 h 20 min under an As overpressure. They observed that for samples grown at $450\text{-}470^\circ\text{C}$, the blueshift is in the 90-95 meV range and it decreases down to 58 meV for the sample grown at 410°C . They attributed this difference to the variation of interface roughening: when the growth temperature increases the QW interfaces become rougher. The roughness can enhance In-Ga interdiffusion during the annealing and this leads to a larger blueshift.

Kim *et al.* [50] also attributed the RTA induced blue shift to the QW intermixing. The samples they studied were InGaAsN/GaAs MQW grown by MOCVD and annealed in the temperature ranged from 650°C to 700°C. Typical annealing times were 30 s. HRXRD results showed an increase in compressive strain. It was supposed that the amount of QW intermixing depends on the concentration of group-III vacancies. The blue-shift in the photocurrent (PC) peak observed at increasing annealing temperature most likely arises from QW intermixing caused by redistribution of intrinsic defects.

Albrecht *et al.* [51] analyzed the influence of annealing on compositional fluctuations in InGaAsN quantum wells (annealed at a temperature of 720°C for 10 min) by means of composition-sensitive [200] dark field (DF) high-resolution transmission electron microscopy and photoluminescence. The annealed samples showed a blueshift of approximately 70 meV.

Their compositional analysis yields two main contributions to the observed blueshift in emission: N diffusion out of the quantum well, and the dissolution of In-rich inclusions present in the as-grown quantum well structures. After annealing, the In profile has changed only slightly. The N concentration profile, however, broadens to 10.3 nm from the 7.4 nm for the as grown sample. In particular, the N concentration in the center of the well is reduced to 2%.

A rough estimation based on published data of quantum wells of the same thickness shows that the main part of the blueshift can be attributed to the reduction in N concentration.

Atomic Rearrangement Many authors attributed the blueshift of the PL emission upon annealing to the rearrangement of the atoms in the alloys. According to the calculations of Zunger *et al.* [52], the different first neighbour configuration around N in the concentrated random alloys will strongly affect the optical properties of the materials.

For example, Tournie *et al.* [45] have investigated by photoluminescence spectroscopy and x-ray diffraction the influence of *ex situ* postgrowth annealing on the properties of a series of dedicated GaInNAs ternary and quaternary quantum wells (QWs) confined by various barrier layers. In contrast with the opinion that the blueshift was caused by a N diffusion out of the QW and/or Ga/In intermixing at the QW/barrier interface, they attributed it to the internal atomic rearrangement in the InGaAsN well layer. Their reasoning:

1. The experimental results showed the occurrence of a blueshift of the GaInNAs QW line even when confined by GaAsN with the same N content, but absence of a shift for GaAsN QWs confined by GaAs.
2. The PL spectroscopy experiments demonstrated that a significant blueshift of the PL line is observed for all GaInNAs quaternary alloy QWs and only for these irrespective of the barrier material.
3. This interpretation was further supported by the x-ray data which demonstrate the absence of any composition change induced by annealing.

Thus, they supposed that during epitaxial growth, the dominant parameter is the co-

hesive energy which promotes the formation of a Ga-rich environment of N. This however resulted in high local strain. During postgrowth annealing, the presence of point defects induced by the low growth temperature then promoted a change of the N-bonding configuration toward a more In-rich environment to reduce the local strain. In turn, this new configuration opened the band gap which resulted in a blueshift of the PL line.

Another example is the work carried out by Kudrawi *et al.* [47]: 2 sets of samples were investigated : a 300 nm-thick $\text{Ga}_{0.942}\text{In}_{0.058}\text{N}_{0.034}\text{As}_{0.966}$ epilayer and GaInNAs/GaAs MQWs.

The MQWs were annealed *ex situ* at 650°C and 750°C for 60 s. The atom interdiffusion is rather small because there was no significant change between XRD fringes found in as-grown and annealed MQWs. The similarity of the XRDs indicates that the shift of QW transitions cannot be attributed to any significant composition or thickness variations in the quantum wells.

In the raman spectra of the GaInNAs layer, two additional peaks associated with the appearance of In-N bonds, at 462.0 and 492.2 cm^{-1} appeared after annealing and their amplitudes increased with the rise in annealing temperature. In contrast, the strength of the Ga-N related peak at 473.6 cm^{-1} decreased, suggesting a considerable redistribution in nitrogen nearest-neighbor bonds towards In-N bonding.

The photoreflectance (PR) results showed an 'effective' blue-shift of the transition and a change in the lineshape in the PR curve after annealing. The complex structure of the PR signal was attributed to the presence of the N-Ga₃In₁ atom configuration, which gave higher bandgap energy than the N-Ga₄ configuration. After annealing at 800°C and 900°C, PR features in the range of 1.00-1.05 eV enhanced significantly while the PR signal at 0.98 eV disappeared completely. Moreover, PR spectra evidently exhibited a double structure separated by 23-28 meV. This splitting has been mainly attributed to the presence of two different environments of N atoms. i.e., N-Ga₃In₁ and N-Ga₂In₂ atom configurations coexist in GaInNAs layers after annealing. It was concluded that the dominant component that caused the total blue-shift of bandgap energy was hang in nitrogen nearest-neighbor environment from Ga-rich to In-rich.

Chauveau *et al.* [53] have used transmission electron microscopy on as-grown and annealed GaInNAs/GaAs heterostructures, and demonstrated that annealing induces a correlated behavior of both In and N species within the GaInNAs quantum well while no intermixing occurs.

The analysis of the strain situation revealed that the main driving force for the observed inward diffusion is not composition gradients at the interfaces, but local strain fields. This mechanism leads to the improvement of the photoluminescence (PL) properties and to the blueshift of the PL peak.

The samples under study were nominally $\text{In}_{0.37}\text{Ga}_{0.63}\text{N}_{0.035}\text{As}_{0.965}$ QWs grown on GaAs substrates by solid-source molecular-beam epitaxy. The *ex situ* annealing was carried out under N ambient at 680°C for 1 h. there is a strong enhancement of the radiative efficiency as well as a blueshift of about 30 meV in the PL emission.

Their results thus demonstrated that no interdiffusion of N nor In was detected between the QW and the barrier during annealing, despite the highest gradients of composition at the QW/barrier interface. In contrast, during annealing, both species diffused inward to the QW in order to homogenize the compositions and generate nearly perfect QW profiles. Finally, the In and N displacements were strongly correlated, and this may be related to the reduction of the local strain generated by the large differences in atomic radii between Ga and In, and between As and N.

Finally, this reorganization within the QW affects the N bonding configuration. Since the N atoms diffused from interfaces, i.e. from Ga-rich areas to an In-rich area in the center, the probability to create an In-rich environment for N atoms was increased. This resulted in a thermodynamically more stable distribution, which can furthermore be responsible for the blueshift of the PL emission.

Kondow *et al.* [46] have also concluded that the annealing induced blueshift in (In)GaAsN materials were caused mainly by the internal atom rearrangement in the material.

In their work, two sets of samples were studied: One structure was a $\text{Ga}_{0.3}\text{In}_{0.7}\text{N}_{0.01}\text{As}_{0.99}$ single quantum well (GaInNAs-SQW), the other was a 100 μm thick $\text{Ga}_{0.95}\text{In}_{0.05}\text{N}_{0.02}\text{As}_{0.98}$ bulk layer. All were grown by molecular beam epitaxy (MBE). *In situ* annealing was carried out in the MBE chamber after crystal growth for 1 h, at temperatures of 500, 550, 600 or 650°C, under an As_2 beam.

The bandgap energy of GaInNAs layers was found to be blue shifted. The rate of increase in bandgap with temperature of annealing was $0.26 \text{ meV}/^\circ\text{C}^{-1}$. They also found that thermal annealing clearly leads to a dramatic improvement in uniformity of the cathode luminescence intensity across the samples.

In the IR spectra for GaInNAs samples, annealed *in situ* in the MBE chamber under an As_2 beam. An annealing under temperatures from 550 to 650°C for 1h, the intensity of the peak at 470 cm^{-1} decreased as the temperature increased. At higher annealing temperature, additional peaks appeared at 460 and 490 cm^{-1} . They also found that the total intensity did not change, and that the intensity of the peak at 460 cm^{-1} was almost independent of the annealing temperature. Thus, as the peak intensity at 470 cm^{-1} decreased, the peak intensity at 490 cm^{-1} increased. This means that the transition from the peak at 470 cm^{-1} to that at 490 cm^{-1} with rising temperature of annealing, probably originates in alternation to the GaN-bond state.

This result maybe due to an internal change in the GaInNAs crystal, i.e. to atomic relaxation. Since the IR-absorption peaks for larger-bandgap semiconductors with smaller bond lengths are generally seen in the region of higher energy, the blue-shifted phonon energy of the GaN bonds indicates shortening of the bonds. The main reason for the red shift in the bandgap of GaInNAs is a volume effect GaInNAs. It was observed that the redshift in the phonon energy of nitrogen-related bonds is proportional to the lattice mismatch between the individual binary crystals and the GaInNAs. Hence, the redshift in the phonon energy of the nitrogen-related bonds can be used as a tentative measure of bond extension in GaInNAs. On this basis, the authors estimated that the GaN bonds corresponding to a TO phonon energy of 490 cm^{-1} are shorter by 24% than

those for GaN bonds corresponding to a TO-phonon energy of 470 cm^{-1} .

When the temperature of annealing is 650°C , the degree of absorption was roughly the same at 470 and 490 cm^{-1} . This indicates that roughly equal numbers of GaN bonds are in the states corresponding to the respective wavenumbers. The GaN bonds corresponding to 490 cm^{-1} were 24% shorter than those corresponding to 470 cm^{-1} . The bandgap of this *in situ* annealed sample was 1.12 eV, which represented a blueshift of 45 meV from the result for the as-grown sample. These results could be keys to an understanding of atomic relaxation in GaInNAs. Thus, they supposed the mechanism responsible for the annealing-induced change in bond length or atomic relaxation in GaInNAs is: Non-radiative centres were present in as-grown GaInNAs; these non-radiative centres were probably point defects, such as vacancies. The migration of point defects may produce a rearrangement of the sites of atoms. During this atomic rearrangement, the elongated GaN bond might made a transition to a lower energy state corresponding to a shorter bond and, thus, the atomic relaxation might be generated. When the point defects were made to wander about and were then extinguished by the annealing, the atomic relaxation may be the means for a transition to a state with lower internal energy.

3.1.2 Red Shift of Optical Emission upon Annealing

Although most of the authors reported blueshifts of the optical emission of (In)GaAsN materials after they had undergone a thermal annealing process, including bulk dilute nitride layer and quantum well (QW) structure, there are a few reports on the redshift of the bandgap energy after annealing of this type of materials.

An example is the work of Francoeur *et al.* [54]. They studied samples of (In)GaAsN layers grown by a custom-designed metal-organic molecular beam epitaxy apparatus. PL changes induced by the annealing for all of the 5 minute anneals, up to 650°C , were a slight redshift of the luminescence peak, about 15 meV for the sample with 0.7% N. They attributed this redshift to the increased nitrogen incorporation, in accordance to their XRD rocking curve measurement results.

3.1.3 No shift of Optical Emission upon Annealing

There are also reports that there is no obvious shift observed after annealing. For example, Rao *et al.* [55] investigated GaAsN layers grown by metal-organic vapor phase epitaxy and annealed for 15 min at 650 and 700°C respectively, under excess As ambient in the epi-reactor. They did not observe an energy shift of the PL emissions in their experiments.

Another report is on the laser annealing treatment carried out by Toivon *et al.* [56]. They compared the different effects of laser annealing and thermal annealing. (The samples were grown by MOCVD and the thermal annealing was carried out *in situ* for 10 min at 700°C in a H carrier gas and excess TBAs ambient. The laser treatments were performed for 1 min with different irradiation intensities.)

The effects of thermal annealing and laser treatment are fairly similar; for the GaAsN

QWs with different N content x , annealing at 700°C for 10 min, the photoluminescence peak shifted by 86 meV toward higher photon energies. For the same quantum well structure under laser treatment, the blueshift of the luminescence peak is negligible.

3.1.4 Comparison of Different Effects Caused by Annealing on (In)GaAsN Materials Grown by Different Methods

Balkan *et al.* [57] investigated the effects of fast and slow annealing on the optical properties of molecular and chemical beam epitaxy (MBE and CBE respectively) grown material, where the latter is likely to contain a higher density of hydrogen impurities as a result of the gaseous precursors and low growth temperatures.

The samples under investigation were grown on GaAs (100) substrates either by CBE or MBE. They were a 7-nm $\text{Ga}_{0.7}\text{In}_{0.1}\text{N}_{0.0355}\text{As}_{0.9645}/\text{GaAs}$ single quantum well (SQW) and a 3-nm $\text{Ga}_{0.7}\text{In}_{0.3}\text{As}/\text{GaAs}$ SQW reference layer. The MBE samples used in this study were grown by plasma-assisted solid-source MBE.

Fast thermal annealing (FTA) was performed by placing the samples into a furnace pre-heated at the required annealing temperature. In slow thermal annealing (STA), the sample was placed on the furnace plate at room temperature and heated gradually to the desired anneal temperature.

The MBE-grown material underwent conventional *in situ* RTA under Ar gas at 650 °C for 30 s. FTA was also carried out on the MBE-grown samples.

The CBE-grown material was annealed (FTA) at several different temperatures between 450°C and 700°C, for a duration of 10 s at each anneal temperature. It is clear that the wavelength red-shifts by about 20 nm in the whole range with the increasing anneal temperature higher than growth temperature.

They proposed that during the hydrogenation process N-H bonds are created within the crystal lattice. This decreases the effective nitrogen concentration and consequently increases the bandgap energy of the quantum well. Post-growth annealing annihilates these weak bonds and, therefore, restores the optical properties of the hydrogen-free GaInNAs material.

In another CBE-grown material, $\text{Ga}_{0.7}\text{In}_{0.3}\text{N}_{0.0125}\text{As}_{0.9875}$, after the FTA the PL intensity increases, FWHM decreases and the peak wavelength remains almost constant. However, the peak wavelength is blue-shifted by 4 nm. This observation supports the existence of two competing wavelength shift mechanisms in this material. When the sample is annealed using FTA, the N-H bonds are rapidly annihilated with the consequent shift of the PL emission towards lower energies. At the same time, indium and nitrogen tend to diffuse out of the QW, causing the PL emission to blue-shift. However, judging by their observations, it appears that FTA favors the former process. The latter process is dominant in the STA.

In the MBE grown samples, irrespective of the anneal technique used, annealing always results in a blueshift compared to the as-grown sample, and a reduction in the FWHM.

After annealing, the PC peak energies corresponding to the e1-hh1 transitions blue-shift by about 20 meV and 10 meV for GaInNAs and GaInAs, respectively. This behavior is in agreement with the PL results and can be explained in terms of the reconfiguration of the nearest-neighbor atoms around nitrogen atoms. Between the Ga₄N and Ga₃InN configurations, it is believed that the main part of the 20 meV blue shift arises from increasing In-N bonds. As the In-N bond is less strained than Ga-N bonds in the GaAs lattice, the blueshift for the GaInNAs/GaAs QW indicates a preference to form In-N bonds instead of Ga-N bonds upon annealing.

They concluded that two effects contribute to the blueshift in the MBE grown samples: redistribution of the nearest-neighbour configuration and quantum well fluctuations due to In-Ga interdiffusion, because they observed both the 4 meV difference in blue shift of the GaInNAs QW relative to the shift caused by the configuration difference between Ga₄N and Ga₃InN and the 10 meV blueshift of the GaInAs QW.

3.1.5 Increase of the Intensity of PL Emission and Investigations on Point Defects Evolution under Post-growth Anneal

Of all the PL studies on the annealing effects on (In)GaAsN, almost all reported an increase in the PL intensity upon annealing and this increase was interpreted as due to the annihilation of point defects. But there are many different types of point defects discussed.

Since all the GaAsN materials were grown under thermodynamically non-equilibrium conditions (because of the miscibility gap between GaAs and GaN), the existence of point defects is a common phenomenon in this group of materials and one of the main reasons degrading the sample quality. One of the purpose of RTA on GaAsN is to annihilate these defects. In the past decades, a number of works on the evolution of point defects during annealing were carried on by several groups:

In the study in ref [48], the PL intensity increases with annealing temperature to a maximum at 750°C for 10 s. The evolution of PL features of a sample as a function of RTA time was also investigated at 750°C. They found that the PL intensity increased in the initial stage of RTA and reached its maximum in 10 s, indicating the defects are quickly removed from the QW. As annealing continues the intensity decreases, probably due to the reduced quantum efficiency of the QWs with degraded interfaces.

According to Rao *et al.* [55], post-growth heat treatments at 650°C lead to higher PL intensity and sharper PL linewidths. They attributed the improvement of PL properties to a complete annealing of nonradiative defects and they supposed that the type of point defects is the N-H complex because:

1. By SIMS, they detected not only H and C but also found them to follow closely the N distribution although at different concentration levels.
2. The fact that the hole concentration of the samples is not far below the concentration of C as measured by SIMS assures that these atoms are free and consequently not complexed with H, despite their known high affinity. That the distribution of H continues

to follow closely that of N in the annealed sample confirms the assumption of complex formation and their apparent thermal stability.

In Tournie's results [45], GaAsN QW PL intensity was improved by one order of magnitude and its linewidth was reduced upon annealing.

Their data demonstrated that the high density of nonradiative recombination centers does not stem from the presence of N, but mainly arise from the very low growth temperature which be used to prevent decomposition of the unstable GaInNAs alloys.

Albrecht *et al.* [51] interpreted the PL intensity increase to the homogenization of the In distribution. These processes result in a reduction of the maximum In concentration and thus in a removal of deep localizing potential fluctuations.

The laser-annealing effects study of Ref. [5] showed that the PL efficiency of the treated samples increases gradually with increasing laser treatment intensity in the range $420\text{W}/\text{cm}^2$ to $10000\text{W}/\text{cm}^2$ and then saturates.

The effects of thermal annealing and laser treatment are fairly similar for a $\text{GaAs}_{0.968}\text{N}_{0.032}$ QW after different post-growth treatments. After annealing or laser treatment, the luminescence intensity is high. The laser-treated sample exhibits twice the intensity of the thermally-annealed sample, and the greatest intensity is obtained when both treatments are implemented.

It is also worth of noticing that in Ref. [57], it is noted that the PL intensity does not appear to increase after annealing, unlike their CBE-grown samples.

Gao *et al.* [58] have studied the evolution of electrically active defects in rapid thermally annealed p-type GaAsN epitaxial layers using deep-level transient spectroscopy (DLTS). Unintentionally p-doped GaAsN epitaxial layers (825 nm thick) were grown by low-pressure metal-organic chemical vapor deposition (MOCVD) on Zn-doped GaAs substrates. The nitrogen composition was estimated to be 0.31%. Rapid thermal annealing (RTA) was performed on the samples in the $600\text{-}900^\circ\text{C}$ range for 30 s in N_2 ambient.

There is a gradual increase in the doping concentration up to 800°C followed by a relative decrease at the higher annealing temperatures. In particular, the annealed p-type layers showed an increase in apparent hole concentration, whereas the opposite effect was observed in annealed n-type layers.

The increase in apparent hole concentration with annealing could be explained by either the removal of N-H bonds and/or the formation of the electrically inactive N-H_2 structure in the annealed samples. Removal of N-H is found not to be the dominant mechanism affecting N_A (free hole carrier concentration). It is supposed that marginally lower N_A above 800°C may result from the thermal instability of N-H_2 and its dissociation into the donor-like N-H structure.

The breaking of some N-H bonds may be enhanced at the higher temperatures, leading to an increase in N_A with the increasing annealing temperature. The removal of excess N (i.e. N interstitials) in annealed samples would result in the loss of N-H bonds. The formation of N-H_2 bonds is predicted to be more energetically favorable than the for-

Defect	E_{active} (eV)	Capture cross section (cm ²)	Comparison with previous results
HA1	0.22±0.02	9×10 ⁻¹⁵	H1(N-related) or Hβ4
HA2	0.32±0.02	9×10 ⁻¹⁴	H2 or HL6 (highly doped layers)
HA3	0.38±0.03	1×10 ⁻¹³	HM7
HA4	0.39±0.03	1×10 ⁻¹⁴	Cu _{Ga}
HA5	0.55±0.03	9×5 ⁻¹⁵	H3(EL2-type) or Fe _{Ga}
HA6	0.78±0.07	1×10 ⁻¹²	Cu _{Ga}

Table 3.1: Electrical properties of the hole traps in rapid thermally annealed GaAsN epitaxial layers grown by MOCVD, and the possible related defects (from reference [58])

mation of N-H at high level. Hence, the formation of N-H₂ bonds in annealed samples will produce less hole compensation, i.e. an increase in the apparent hole concentration.

Rapid thermal annealing (RTA) in the temperature range 600-900°C created six hole traps: HA₁ ($E_V + 0.22$ eV), HA₂ ($E_V + 0.32$ eV), HA₃ ($E_V + 0.38$ eV), HA₄ ($E_V + 0.39$ eV), HA₅ ($E_V + 0.55$ eV), and HA₆ ($E_V + 0.78$ eV). Most of these defects are stable at 900 °C. The supposed origin of these defects is listed in Table 3.1.

Ramstainer *et al.* [59] detected nitrogen-related defects in diluted GaAsN by Raman scattering in resonance with the localized E1 transition. The samples investigated were grown by solid-source molecular beam epitaxy using rf plasma sources for nitrogen supply: GaAsN layers of 200 nm thickness and GaAsN MQWs. The samples were treated by rapid thermal annealing (RTA) in the temperature range of 650-950°C.

Two additional peaks at 409 cm⁻¹ and 427 cm⁻¹ were observed in the Raman Resonance spectroscopy, whose integral intensity is related to the N concentration. Since their frequencies are in the range of those found for local vibrational modes (LVMS) of ²⁸Si on Ga (Si_{Ga}) and As (Si_{As}) sites in GaAs, and N₂ molecules have the same atomic weight as ²⁸Si, these two modes were attributed to N dimers on Ga site (NN_{Ga}) and As site (NN_{As}), respectively.

Thinh *et al.* [60] have also studied the point defects by optically detected magnetic resonance technique.

7 period GaAs/GaN_xAs (MQW) structures and 1100 nm thick GaNAs epilayers were grown by gas-source molecular beam epitaxy (MBE).

The N composition x in the structures was varied from 1.2% up to 4.5%. RTA was performed at 850°C for 10 s. The samples were investigated by magnetic resonance technique. Defect related peaks were observed in the experimental results. The results revealed that the g value for both defects is isotropic and close to 2, implying that they are deep defects. One of them was identified as an As-Ga antisite defect.

Postgrowth RTA can significantly suppress the influence of the nonradiative defects studied, and can be accompanied by a dramatic improvement in the efficiency of the light emission.

3.1.6 Electronic Properties Evolution under Post-growth Annealing

Post growth annealing was also found to introduce type conversion in InGaAsN alloys in the works of Kurtz *et al.* [61].

The as-grown samples were p-type, but showed n-type character after less than 15 min. of annealing. The electron concentration increased with anneal time, saturating at about $3 \times 10^{17} \text{ cm}^{-3}$. The electron mobility showed a similar increase with anneal time.

SIMS measurements on the 1 eV GaInNAs grown with TMGa and DMH demonstrated that only H and C showed concentrations greater than the observed electron concentrations. Although C is a p-type dopant in GaAs, if it were located on the group III site in GaInNAs it is not implausible that C could act as an n-type dopant. Annealing could cause the movement of C from the group V to the group III site, causing the type conversion. To investigate this possibility they selected Ga and N precursors that are known to decrease the carbon incorporation.

The authors found that the electron concentration was roughly proportional to the H concentration for this set of samples. They proposed that H may act as a donor in their samples. Also because their experimental results is in qualitative agreement with other theoretical predictions. [62–64]

3.2 Previous Investigations of Annealing Effect on Other Semiconductor Materials

Constantinos Christofides *et al.* have made systematic investigations on the annealing effects on implanted Si wafers. Here we summarize some of their main results and conclusions:

One important work is to monitor the kinetics of thermal annealing on these implanted silicon wafers by studying the dependence of the photothermal reflectance (PTR) signal on annealing conditions [65].

The samples under study consisted of silicon wafers implanted through an oxide layer with P^+ ions at different doses.

Upon removal of the SiO_2 overlayer, some of the samples were thermally annealed isochronally (1h 20 s) under different temperatures (400, 500, 600 and 800°C).

The authors found that high temperature annealing led to annihilation of the P^+ induced damage for doses higher than 10^{15} ions/cm s.

They also found that annealing at a relatively low temperature of 400°C caused a noticeable decrease of the PTR signal, implying a significant decrease on local disorder, which was attributed to annihilation of many kinds of point defects such as interstitial vacancy, arsenic vacancy, and divacancies. (The various defects induced by ion implantation, the required annealing temperature for their annihilation and the corresponding activation energy are listed in Table 3.2).

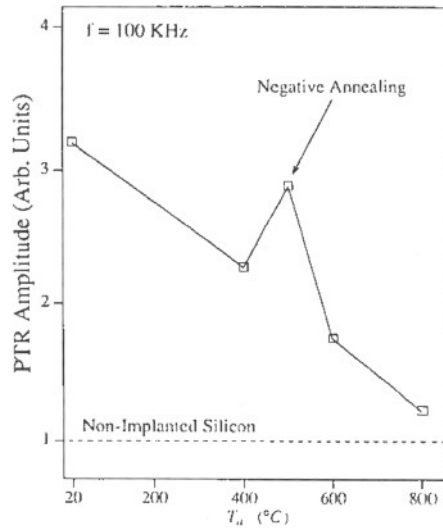


Figure 3.1: Variation of the photoreflectance signal as a function of annealing temperature for arsenic-implanted silicon wafers(from reference [65])

Type of damage	T_a (°C) t=30-60 min	E_a (eV)
Interstitial vacancy	180	0.2-0.5
Arsenic vacancy	200	0.8
Divacancy	300	1
Layer completely "amorphous"	550-650	2-3
Layer incompletely "amorphous"	700	3-4
Line dislocations	800-1000	5-8
Loop dislocations	800-1000	5-8

Table 3.2: Defects induced by ion implantation, required temperatures for their annihilation, and the corresponding activation energies (from reference [66])

There was an increase of the PTR signal between 400 and 500°C, which may be associated with the formation of arsenic complexes (shown in Fig. 3.1). This phenomenon is known as negative or retrograde annealing. It occurs when the concentration of impurities in the damaged host lattice is sufficiently high to promote their migration toward each other as the annealing temperature is raised. Higher annealing temperatures (higher than 550°C) were required to dissociate these arsenic defects. For high annealing temperatures (higher than 600°C), the signal approached that of the non-implanted silicon, indicating a high degree of crystallinity restoration. In fact, only line and loop dislocations could survive after annealing at 800°C.

In reference [67], the authors presented photoluminescence results obtained from phosphorus-implanted silicon wafers lightly doped with boron.

The wafers were implanted with phosphorus at various doses through a thin oxide layer at room temperature and then annealed isochronically at various temperatures from 300 to 1100°C for 1 h in an inert nitrogen atmosphere.

It appears that the PL curves could be divided into three well defined annealing temperature stages: 300-400; 400-700; and 700-1100°C. In the first range (300-400°C), the PL signal increases drastically with annealing temperature especially for the high implanted samples. This is caused by annihilation of defects in this range.

In the range 400-700°C, they note that the luminescence has a large dip around 600°C. That is the negative annealing, which is due to the formation of complex defects around this annealing temperature; thus the majority of carriers are trapped. Annealing from 700 to 1100°C results in a decrease of the luminescence, reaching a negligible value at the highest annealing temperature.

The PL signal reaches a maximum at 750°C and then decreases again with increasing annealing temperature. The similar behavior of the luminescence for all three samples around this maximum seems to suggest that this feature is mainly due to the implantation itself rather than the lattice defects caused by implantation damage.

The authors supposed that the decrease in luminescence at the highest annealing temperature is probably due to the same reason as in the reduction of luminescence of laser annealed non-implanted silicon samples in Ref. [68], i.e., deep level defects caused by the annealing processes.

The authors also employed [66] a kinetic model based on four coupled differential equations to study the carrier kinetics during thermal annealing on implanted silicon wafers .

The samples used in the experiments were silicon wafers lightly doped with boron implanted with phosphorus through a thin oxide layer. These samples were then thermally annealed isochronically at various temperatures: 350, 400, 500, 600, 700, 800, 900, 1000 and 1100°C for 1 h. under inert nitrogen atmosphere.

The annealing process of the implanted silicon, even as low as 350°C, induces a great deal of change in the carrier lifetimes. The lifetime of the photogenerated carriers increased to 8.9 psec as the recombination traps are annealed and removed. This takes

place due to the annihilation of point defects.

The carrier lifetime increases further with increasing annealing temperature up to 400°C whereas the signal is decreasing. The drop in carrier lifetime in the 500°C sample is believed to be due to the formation of complex clusters as the implanted samples are annealed ("negative annealing"), the impurities diffuse into the bulk forming clusters, which act as recombination centers and traps to the photogenerated carriers.

Around 700°C, complex defects annihilated, resulting in an increase of carrier lifetime. Nevertheless, at higher annealing temperatures 900°C, dislocation lines and loops become an important recombination mechanism for the carriers generated following ultrafast-pulse photoexcitation, which results in a decrease in carrier lifetime. A further increase in the annealing temperature removes the dislocation lines and loops, resulting again in an increase in carrier lifetime. Specifically, a change of annealing temperature from 900 to 1100°C results in an increase of carrier lifetime from 19.6 to 95 ps.

